Supplementary Information

Temperature Dependence of Anomalous Protonic and Superprotonic Transport Properties in Mixed Salts Based on CsH_2PO_4

Andreu Andrio,[a] S. I. Hernández,[b] C. García-Alcántara,[b] L. F. del Castillo,[c] Vicente Compañ,[d] Iván Santamaría-Holek*[b]

a. Departamento de Física. Universitat Jaume I.12080-Castellón (Spain).
b. Unidad Multidisciplinaria de Docencia e Investigación-Juriquilla, Facultad de Ciencias, Universidad Nacional Autónoma de México (UNAM), Juriquilla, Querétaro, CP 76230, Mexico.
c. Departamento de Polímeros, Instituto de Investigaciones en Materiales, Universidad Nacional Autónoma de México (UNAM), Ciudad Universitaria, Apartado Postal 70-360, Coyoacán, Ciudad de México, 04510.
d. Departamento de Termodinámica Aplicada. Universidad Politécnica de Valencia, C/Camino de Vera s/n, 46022-Valencia (Spain).

(*) Corresponding author. Email: isholek.fc@gmail.com

In this supplementary information we include SEM, EDX and DSC analysis of the samples studied in the present work. Also we incorporate additional information and graphics to complement the study in the main text

Experimental section

The morphology of the samples CsP, CsP-Ba, CsP-Rb, and CsP-S was examined using a scanning electron microscope (SEM) Quanta 200 FEG-ESEM (FEI Company) coupled to an Energy Dispersive X-Ray spectrometer (EDX) for elemental analysis of Cs, P and Ba, Rb, and S, operating at an acceleration voltage of 15 kV, pressure at 60 Pa and low vacuum. Samples were prepared by depositing few mg of powder sample on top of a carbon support.

SEM and EDX analysis

In Figs. S1-S4 the SEM images and EDX analysis of the sample CsP, CsP-Ba, CsP-Rb and CsP-S are on display. With the atomic % of Cs and P and Ba, Rb and S we can compute the chemical composition of every sample. For the case of CsP the atomic ratio between Cs and P, in agreement with Fig. S1 is 1/1.02 that matches accurately to the chemical formula CsH_2PO_4.

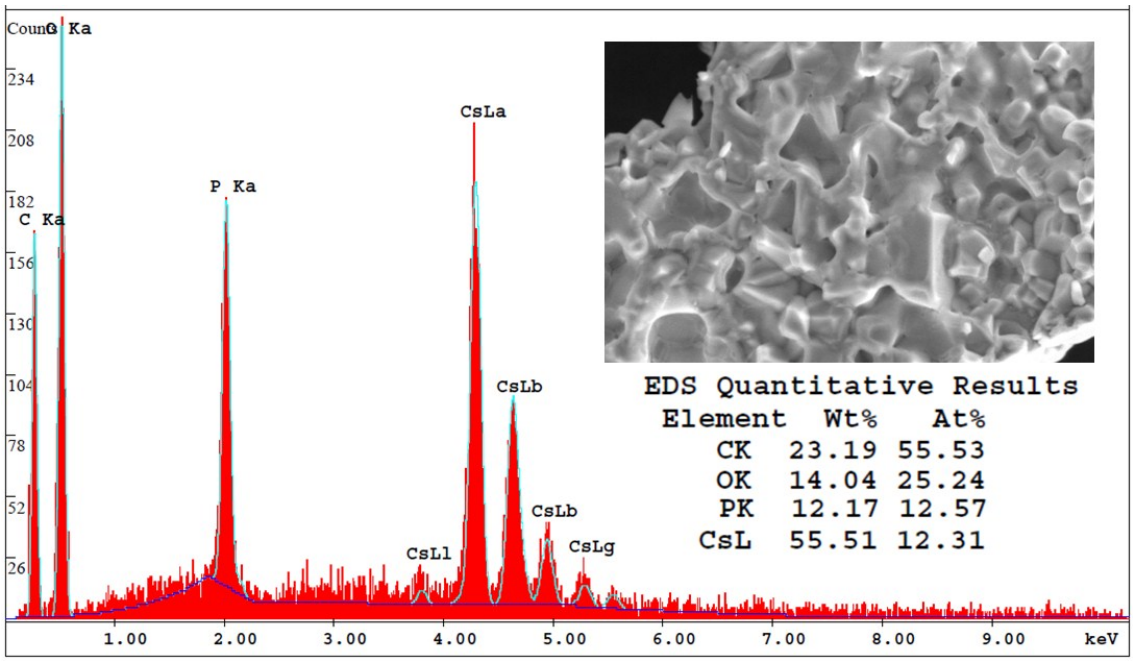

Fig. S1. SEM image and EDX analysis of the sample CsP.

For CsP-Ba the atomic ratios Cs/P and Ba/P are 0.66 and 0.36, respectively that corresponds to a mix of CsH_2PO_4. 0,5 $BaHPO_4$, (see Fig. S2).

A similar situation is encountered for CsP-Rb where ratios Cs/P and Rb/P are 1.07 and 0.28, (see Fig. S3) giving a formula $0.8Rb(H_2PO_4).(Cs_2(HPO_4).(Cs(H_2PO_4)$.

For CsP-S the atomic ratios according to EDX, (see Fig. S4), are Cs/P= 51 and Cs/S= 1.85 of the mixtures of Cs_2SO_4 and CsH_2PO_4 with the addition of H_2SO_4. This result suggest that compound CsP-S will be basically made of Cs_2SO_4 with some impurity due to CsH_2PO_4. The best fit corresponds to 0.96 Cs_2SO_4· $0.04CsH_2PO_4$, in agreement with the concentrations of initial components of CsH_2PO_4 and $CsHSO_4$.

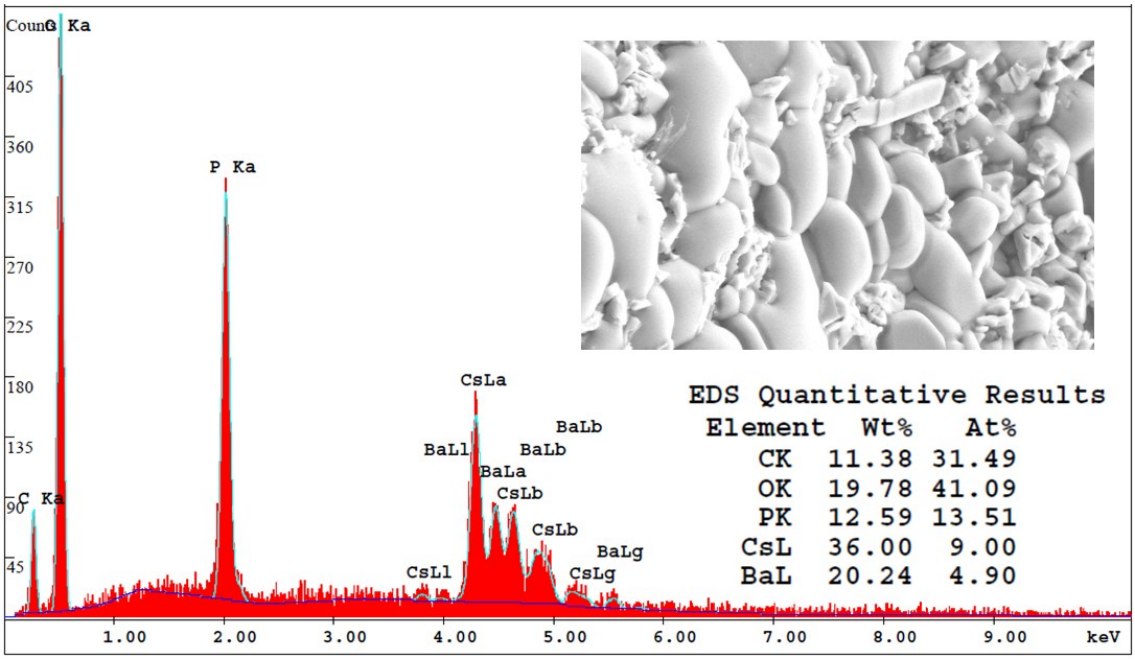

Fig. S2. SEM image and EDX analysis of the sample CsP-Ba.

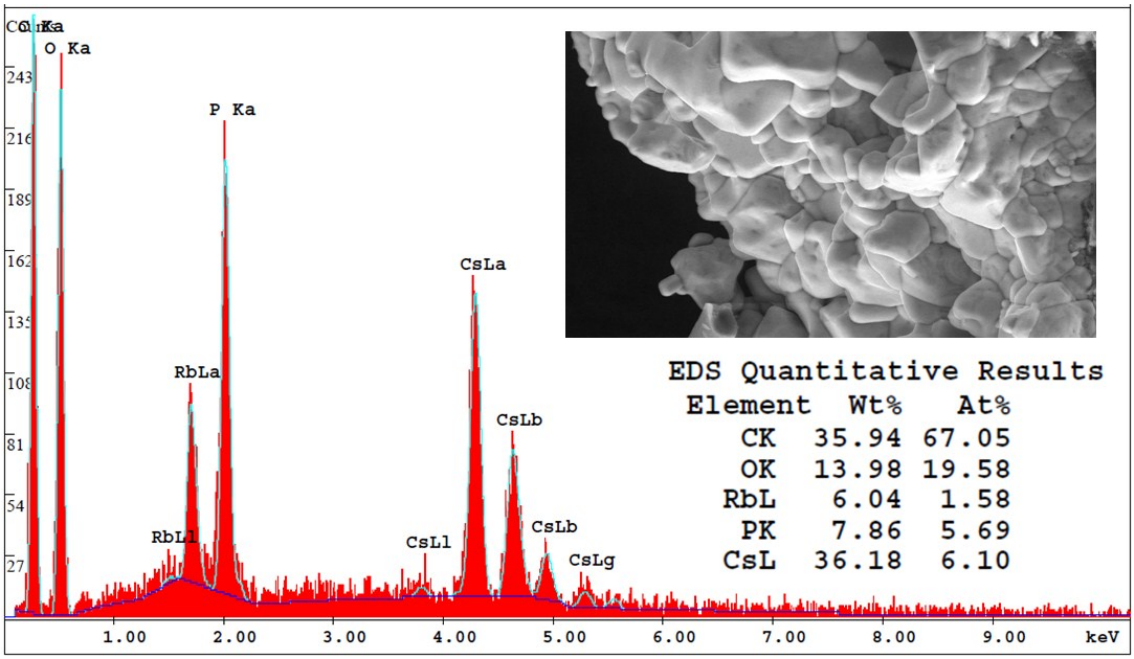

Fig. S3. SEM image and EDX analysis of the sample CsP-Rb.

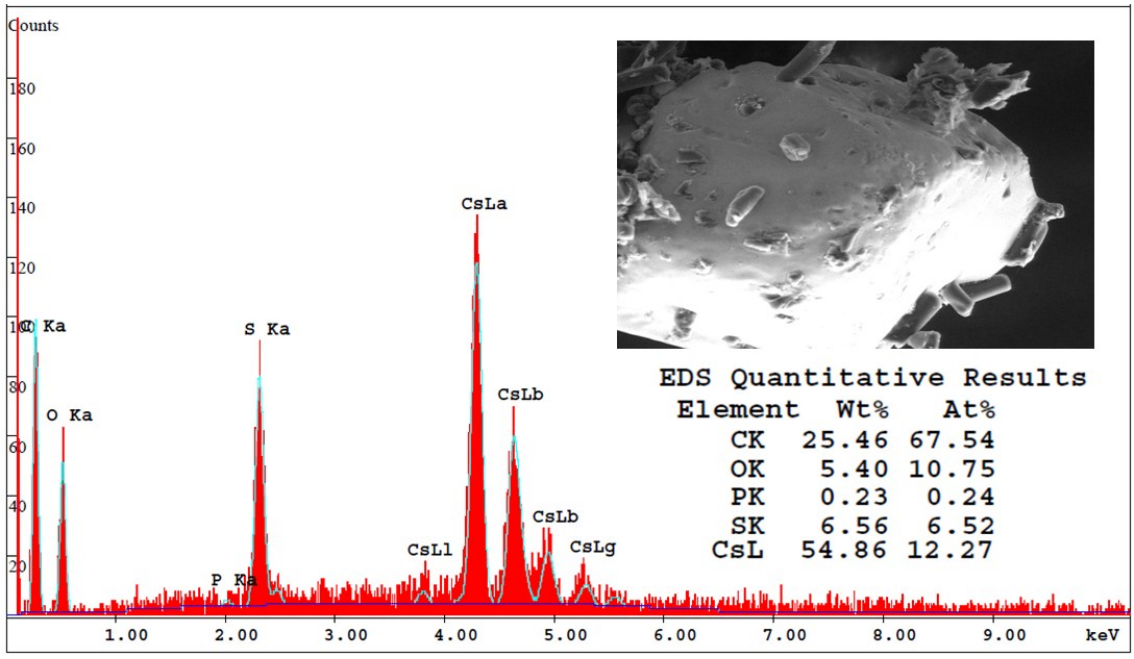

Fig. S4. SEM image and EDX analysis of the sample CsP-S.

The apparent reproducibility of the dependence of conductivity in repeated heating and cooling cycles for initial CsH_2PO_4 in the high temperature (HT) phase is shown in the values of conductivity which differs quasi-one order of magnitude, when the differences between first run and third run are considered. However, when we compares the following runs we observe that these differences tend to stabilize and are practically similar to that observed in the third run. Therefore, we have estimated as adequate this measure for the values of conductivity in our work. In Fig. S5 we can see that reproducibility of measurements is not bad when the first heating and cooling is neglected, and we observe that after the third run the conductivity tends practically to a constant value.

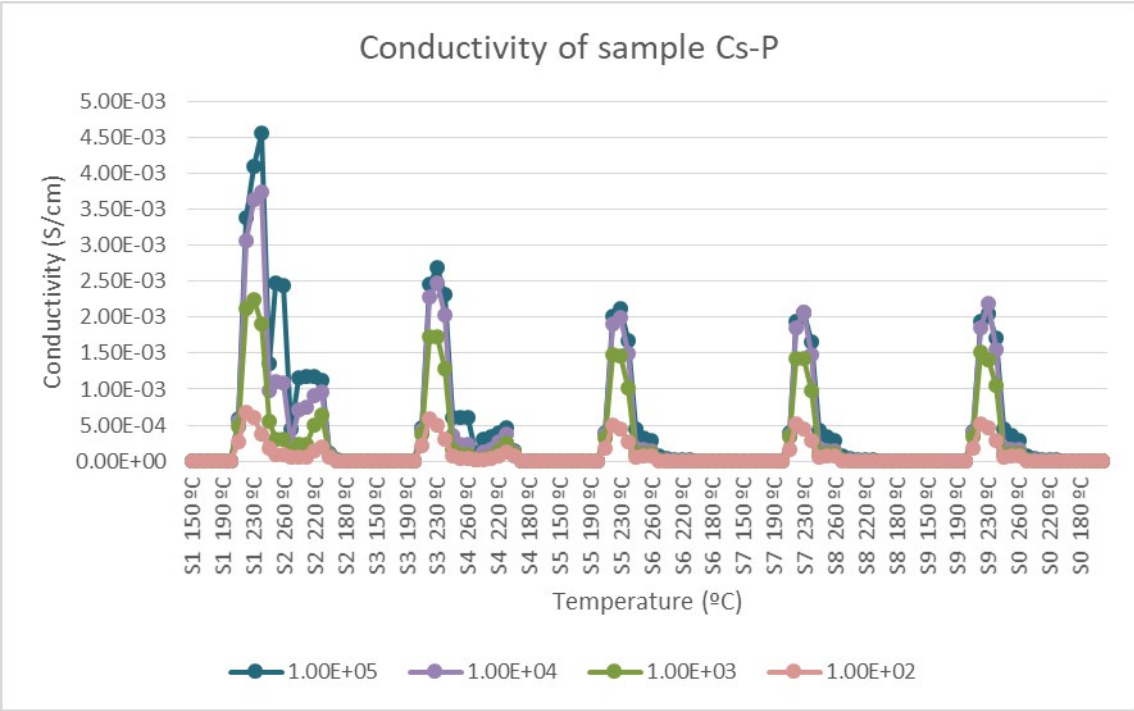

Fig. S5. Variation of Conductivity with temperature obtained for the sample Cs-P at different frequencies (10^5 Hz, 10^4 Hz, 10^3 Hz, 10^2 Hz).

Real part of the conductivity for CsP-S sample

The Bode diagram on Fig. S6 corresponds to the real part of the conductivity of the CsP-S sample in which we can observed the superprotonic transition between 130 and 140°C. The range on temperatures was broaden in comparison to the corresponding Fig. 1 in the main text.

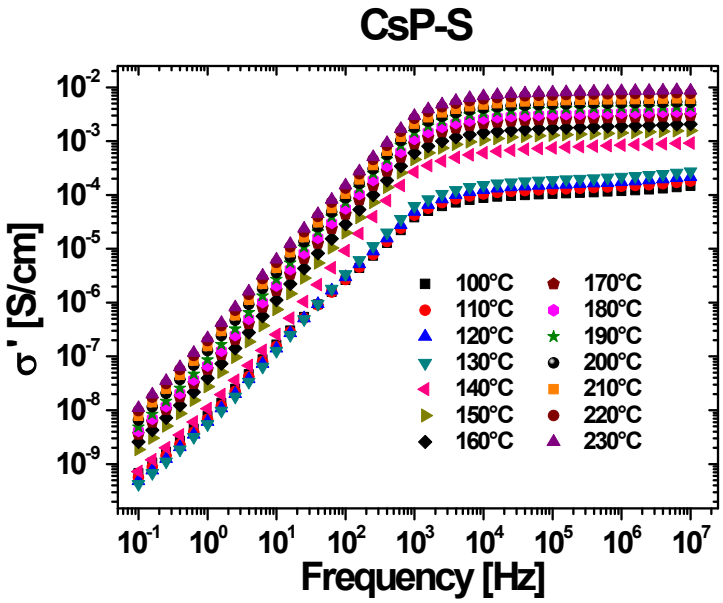

Fig. S6. Bode diagram for the real part of the conductivity in the temperature range from 100°C to 230°C for CsP-S sample. We can observed the jump in conductivity between 130 and 140°C.

Complex dielectric permittivity and tan δ

The plots of ε', ε" and loss tan δ as a function of the frequency for CsP and CsP-Rb show a similar behaviour of the CsP-Ba sample, as stated about the Fig. 2 in the main text.

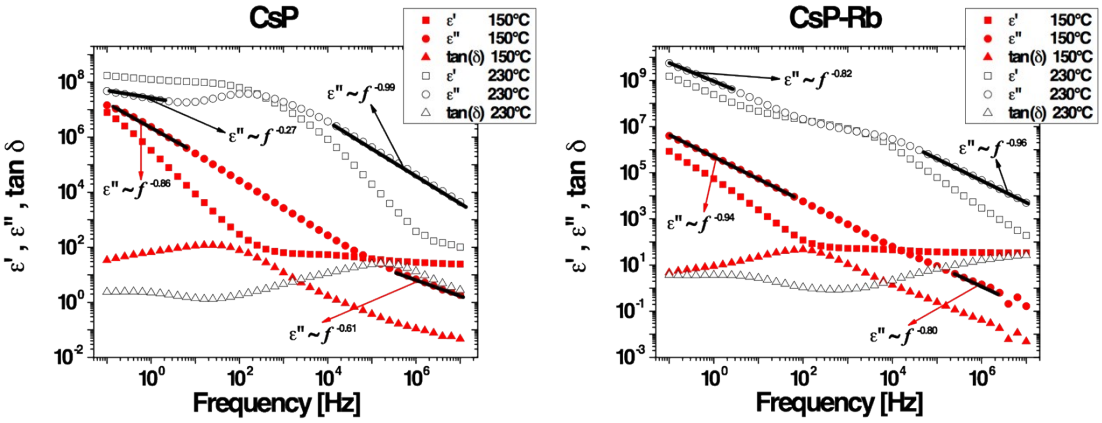

Fig. S7. Real part ε' (squares) and imaginary part ε" (circles) of the complex dielectric permittivity ε*, and loss tan δ (triangles) for two samples at several temperatures. Left: CsP sample at 150°C and 230°C. Right: CsP-Rb sample at 150°C and 230°C.

Cole-Cole and Debye fitting of tan δ

The fit of Cole-Cole model to tan δ data is better compared to the fit with Debye model, as a result of the memory effects in the former. This behavior is similar to that shown in Fig. 5 in the main text for CsP and CsP-Rb.

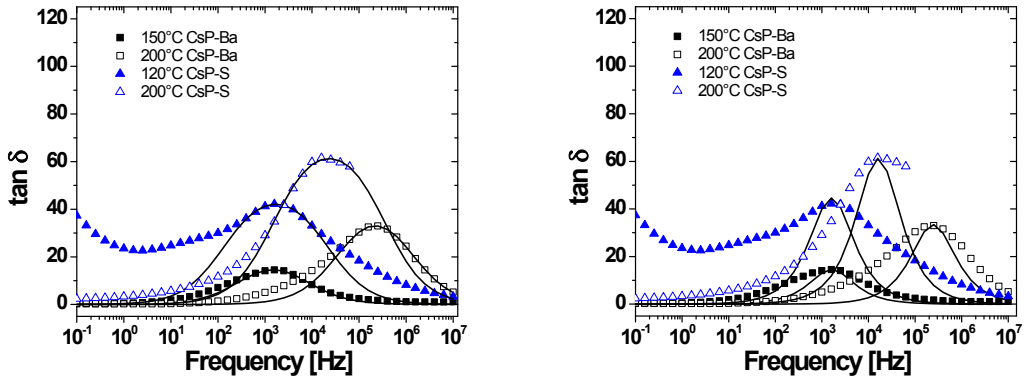

Fig. S8. Tanδ as a function of the frequency at 150°C and 220°C for CsP-Ba (squares), and at 120°C and 200°C for CsP-S (triangles). The solid lines indicate the convolution of eqn (5) in the peak of tanδ at higher frequencies with Cole-Cole model (left), and Debye model (right).

Imaginary part of conductivity

Plots of σ" versus frequency showing the maximum and minimum used to calculated ε_s from Serghei expression (eqn 16 in the main text).

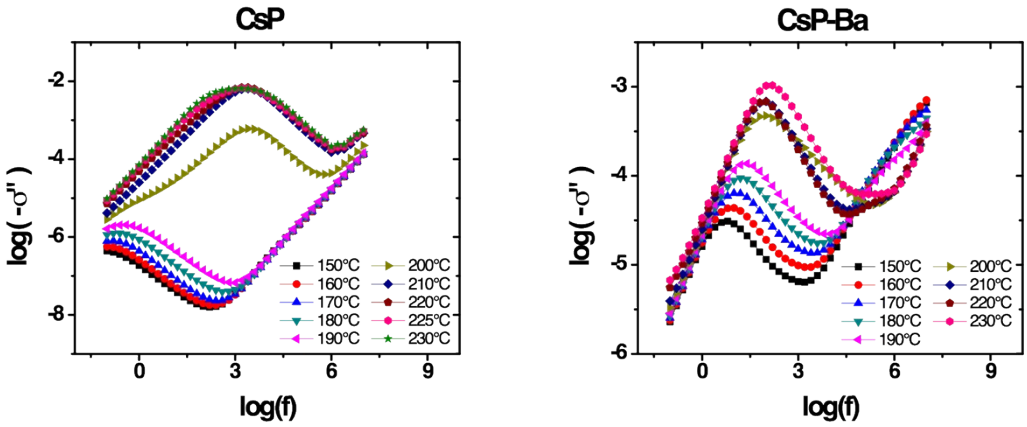

Fig. S9. Double logarithmic plot of σ" versus frequency in the complete range of temperatures studied for CsP and CsP-Ba.

Thermal analysis. DSC

The next figures correspond to the DSC analysis for the samples CsP, CsP-Ba, CsP-Rb, and CsP-S. Each figure shows the presence of polymorphic transitions for each sample. The CsP and CsP-Rb only show the corresponding transition at temperatures around 230ºC corresponding with the SPT and consistent with the results reported in the main text. The CsP-Ba case shows a small absorption window that seems to be correlated with the polycrystalline effects indicated by the Nyquist diagram below in Fig. S11. As expected, the CsP-S compound shows a markedly polymorphic transition near 140ºC, corresponding with the SPT and a second absorption window about 220ºC, again suggesting the possibility of a polycrystalline effect that does not affects the thermal and frequency behavior of the conductivity in appreciable form, as follows form Figs. 1 and 3 of the main text. Our interpretations is that these high temperature windows for CsP-Ba and CsP-S seem to be associated with the emergence of grain polydispersity.

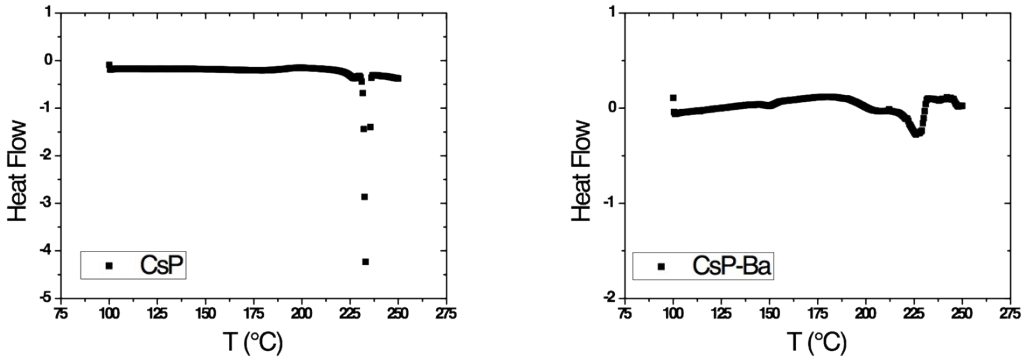

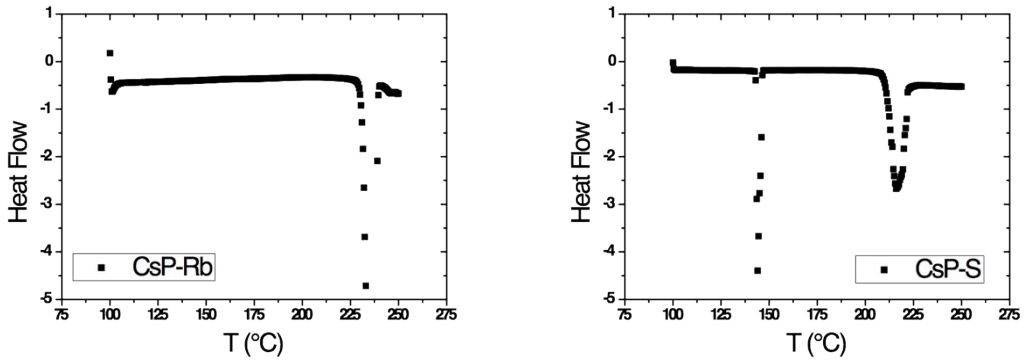

Fig. S10. DSC analysis for the samples CsP, CsP-Ba, CsP-Rb, and CsP-S, respectively.

Nyquist diagrams

In the Nyquist diagram of the samples is not clear the appearance of two semicircles which are associated to polycrystallinity, therefore we conclude that it is not evident such effect.

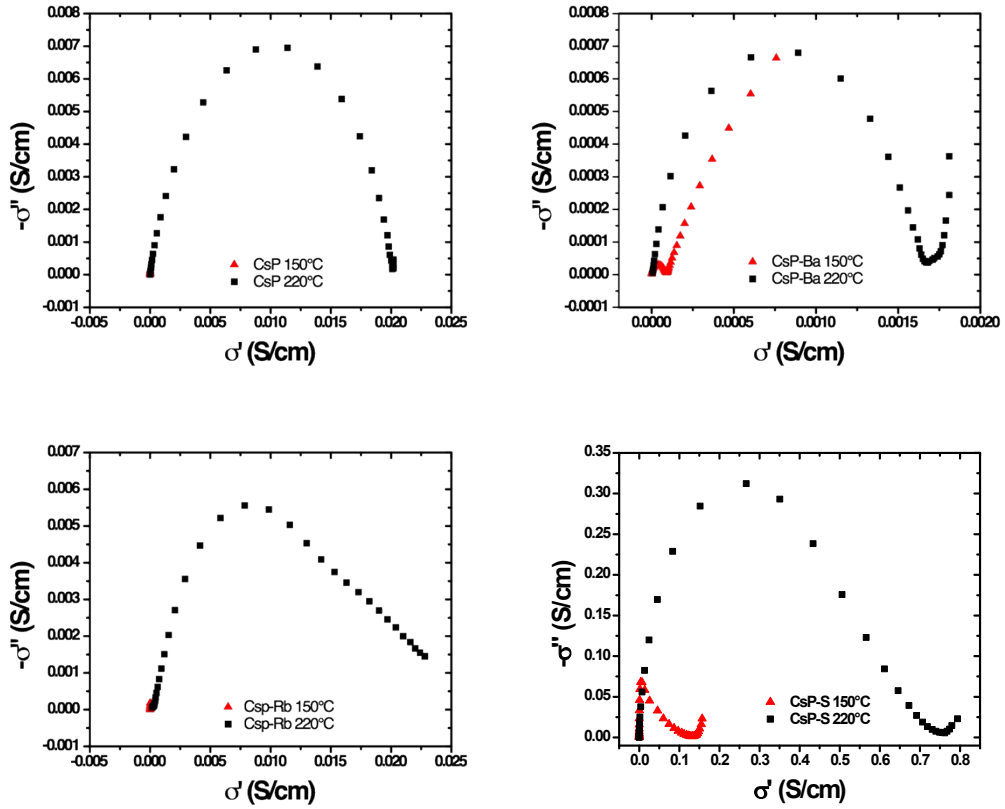

Fig. S11. Nyquist diagrams for the samples CsP, CsP-Ba, CsP-Rb, and CsP-S, respectively.

Fitting the imaginary dielectric permittivity

The analysis of the dielectric spectrum can be performed by fitting both the tanδ as we proceed in the main text by directly fitting the dielectric permittivity. Using the tanδ has the advantage that the effect of conductivity at low frequencies is diminished whereas its presence in the dielectric permittivity makes difficult the identification of the permittivity maximum.

To clarify this point we can see that the conductivity term in eqn (5) of the main text has been neglected, because it is numerically very small[1]. Moreover, since the maximum in the dielectric loss is located at higher frequencies respect to the maximum of ε", it is an advantage to fit the model (i.e. Cole-Cole) to dielectric loss data, because the measurements at low frequencies are generally more difficult[2]. The conductivity term can have a very important effect in the complex permittivity, in such a way that the position of the peak in ε" can be hidden. In contrast, as we have mentioned, the effect of conductivity is diminished in tanδ, facilitating a better fit of the data.

Nevertheless, in order to have a full description, we show in the following figures the fits of the imaginary part of the complex dielectric permittivity with the Cole-Cole model eqn (6), for all the samples at several temperatures, with the parameters of Table 3a, that is, those obtained by fitting the tanδ.

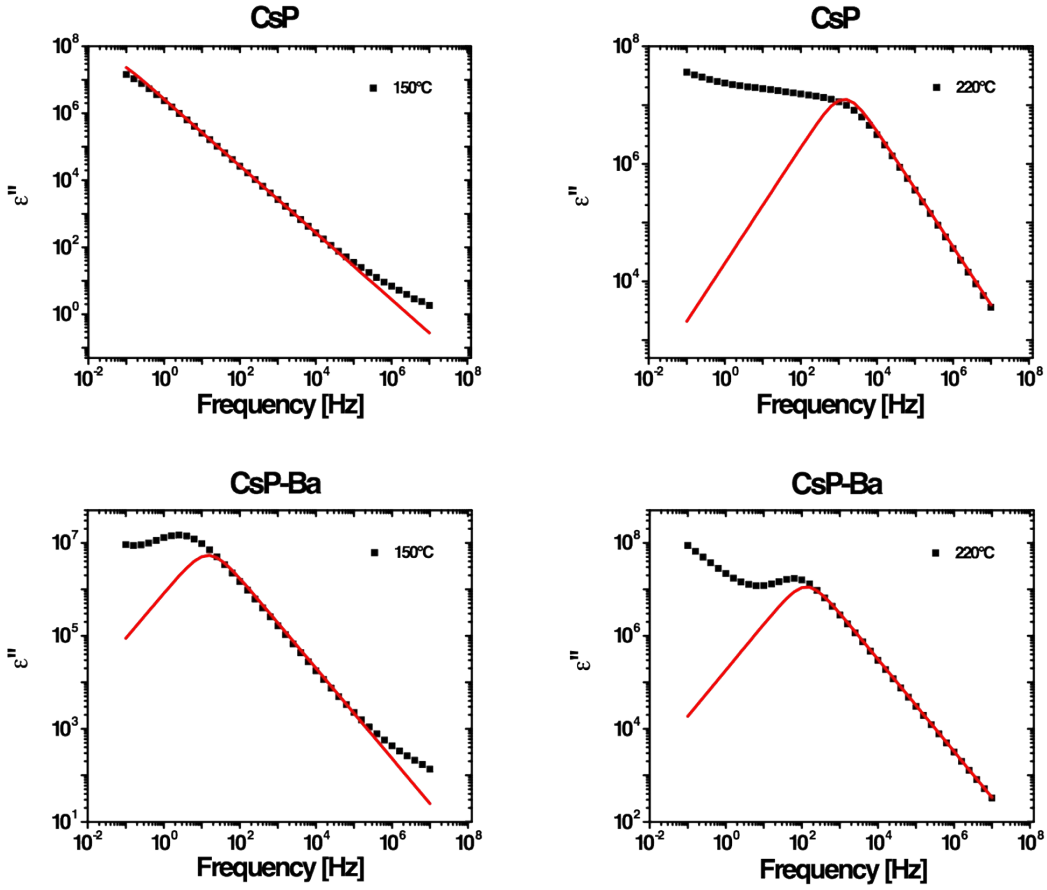

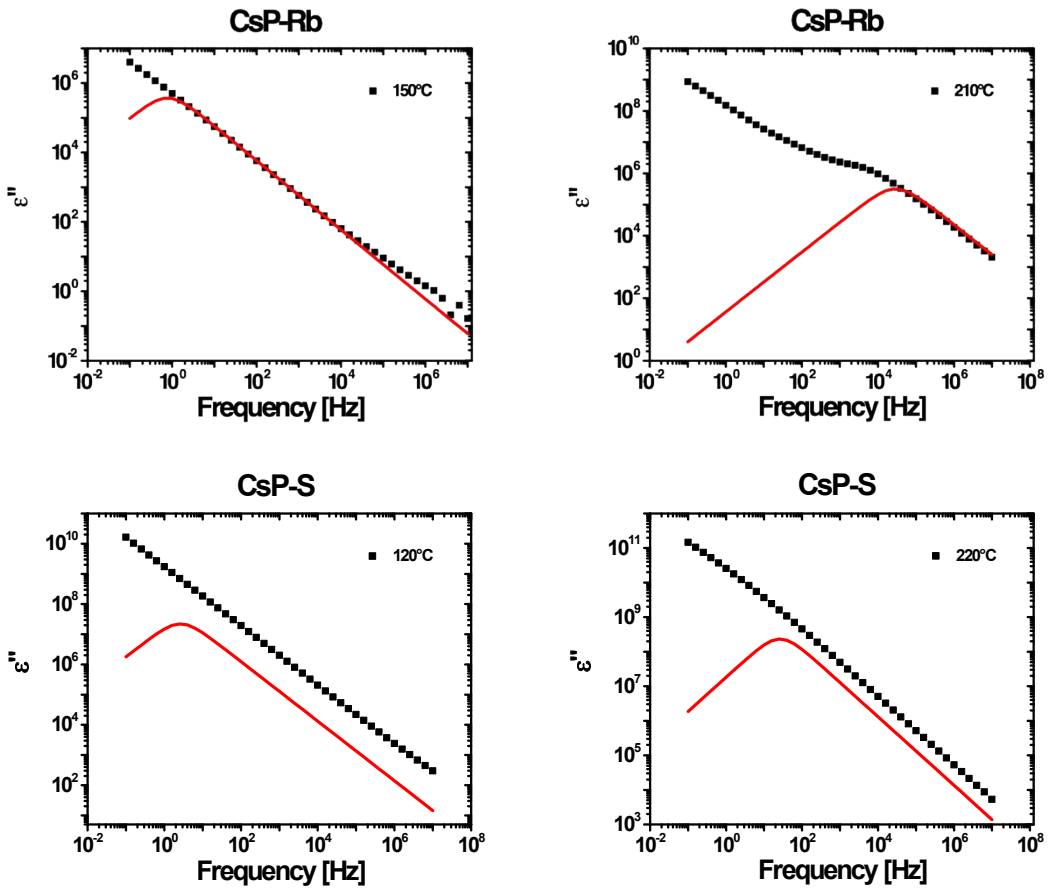

Fig. S12. Fitting the imaginary part ε" of the complex dielectric permittivity ε* with the Cole-Cole model eqn (6), for all the samples at several temperatures. Parameters are from Table 3a which were obtained by fitting the tanδ.

Aknowledgements

We gratefully acknowledge to Profs. Dr. Françesc Teixidor and Dr. Clara Viñas for technical assistance in SEM image and EDX analysis and preparation of samples for such study.

References

1 R.J. Klein, S. Zhang, S. Dou, B.H. Jones, R.H. Colby, J. Runt, *J. Chem. Phys.* 2006, **124**, 144903.
2 T.S. Sørensen, V. Compañ, *J. Chem. Soc., Faraday Trans.* 1995, **91**, 4235-4250.